Chemical and Isotopic Compositions of Hydrothermal Fluids at Snail, Archaean, Pika, and Urashima Sites in the Southern Mariana Trough

45

Tomohiro Toki, Jun-ichiro Ishibashi, Takuroh Noguchi, Miki Tawata, Urumu Tsunogai, Toshiro Yamanaka, and Kentaro Nakamura

Abstract

Hydrothermal fluids were collected from five hydrothermal fields around the Southern Mariana Trough backarc spreading center for chemical and isotopic analyses. Yamanaka site was interpreted as inactive, so we present results from Snail, Archaean, Pika and Urashima sites. The slightly low pH and negative alkalinity suggests a little bit input of magmatic volatiles, supported by high CO_2 concentrations. Consequently low pH would lead to the hydrothermal fluids rich in Fe compared to the MOR hydrothermal fluids.

Keywords

Backarc spreading center • Geochemistry • Hydrothermal fluid • Iron TAIGA • Magmatic volatile • Southern Mariana

45.1 Introduction

The southern part of the Mariana Trough is an active backarc spreading center that had propagated southward (Fig. 45.1a) (Fryer 1995). Several hydrothermal fields have been mapped around 12°50′N in an alignment perpendicular to the spreading axis (Fig. 45.1b) (Wheat et al. 2003; Ishibashi et al. 2004; Utsumi et al. 2004; Kakegawa et al. 2008; Nakamura et al. 2013). This area is far from continents and large islands, so terrestrial organic matter is absent, and the primary production in surface seawater is poor. On the seafloor, sinking organic matter is very sparse, but flourishing ecosystems are sustained around hydrothermal fields despite high temperatures and pressures (Deming and Baross 1993; Takai and Horikoshi 1999; Kelley et al. 2002). Ecosystems utilizing Fe for energy have been extensively documented, especially around low-temperature hydrothermal vents (e.g., Boyd and Scott 2001; Edwards 2004; Edwards et al. 2003,

The online version of this chapter (doi:10.1007/978-4-431-54865-2_45) contains supplementary material, which is available to authorized users.

T. Toki (✉)
Department of Chemistry, Biology and Marine Science, Faculty of Science, University of the Ryukyus, 1, Senbaru, Nishihara, Okinawa 903-0213, Japan
e-mail: toki@sci.u-ryukyu.ac.jp

J.-i. Ishibashi
Department of Earth and Planetary Sciences, Faculty of Sciences, Kyushu University, 6-10-1, Hakozaki, Fukuoka 812-8581, Japan

T. Noguchi
Marine Technology and Engineering Center (MARITEC), Japan Agency for Marine-Earth Science and Technology (JAMSTEC), 2-15, Natsushima-cho, Yokosuka 237-0061, Japan

M. Tawata
Department of Physics and Earth Sciences, Faculty of Science, University of the Ryukyus, 1, Senbaru, Nishihara, Okinawa 903-0213, Japan

U. Tsunogai
Graduate School of Environmental Studies, Nagoya University, D2-1(510), Furo-cho, Chikusa-ku, Nagoya 464-8601, Japan

T. Yamanaka
Graduate School of Natural Science and Technology, Okayama University, 1-1, Naka 3-chome, Tsushima, Kita-ku, Okayama 700-8530, Japan

K. Nakamura
Precambrian Ecosystem Laboratory (PEL), Japan Agency for Marine-Earth Science and Technology (JAMSTEC), 2-15, Natsushima-cho, Yokosuka 237-0061, Japan

Present address: Department of Systems Innovation, School of Engineering, The University of Tokyo, 7-3-1 Hongo, Bunkyo-ku, Tokyo 113-8656, Japan

J.-i. Ishibashi et al. (eds.), *Subseafloor Biosphere Linked to Hydrothermal Systems: TAIGA Concept*,
DOI 10.1007/978-4-431-54865-2_45,

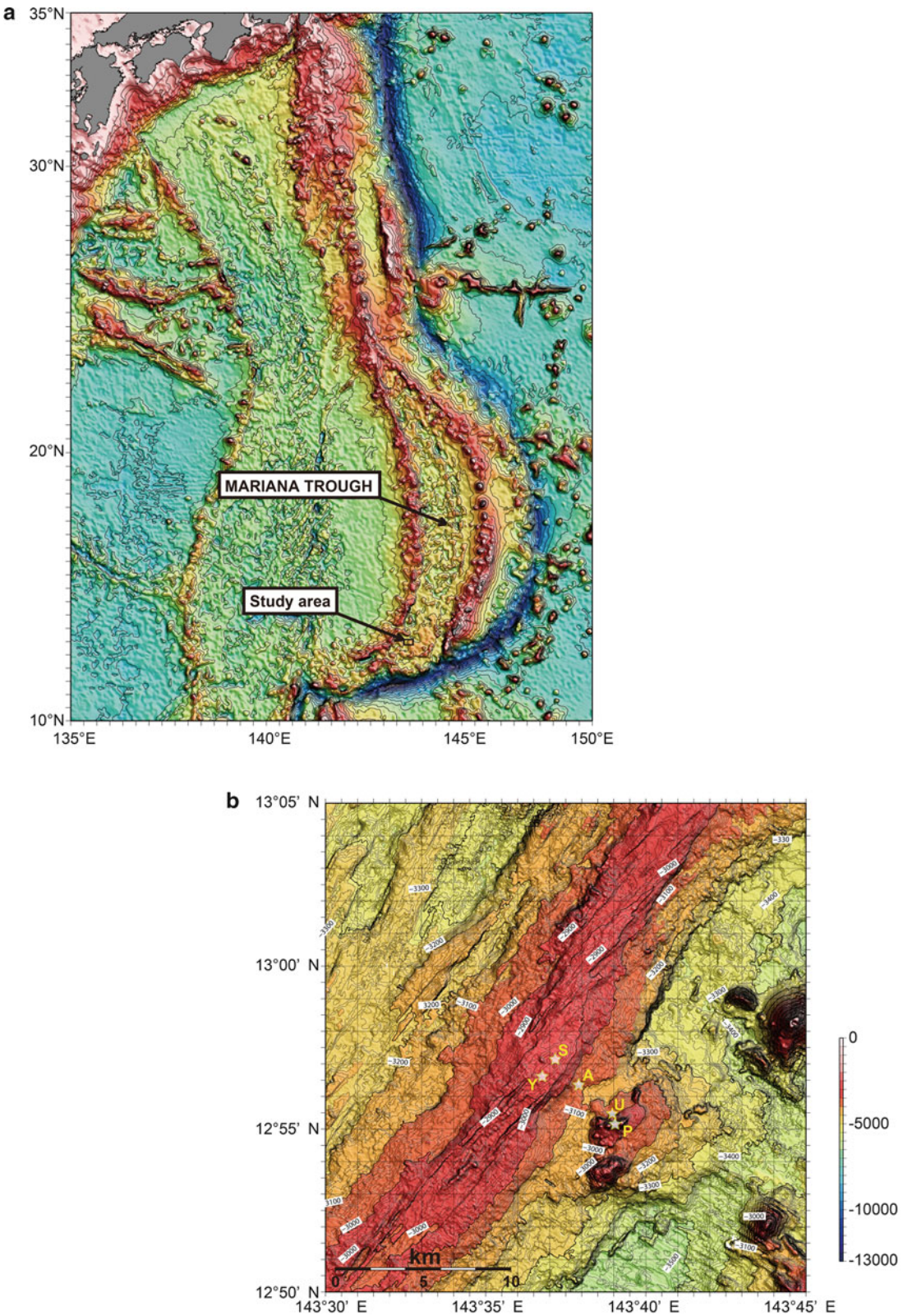

Fig. 45.1 (**a**) A topographic map showing the Izu-Bonin-Mariana trench/arc/back-arc system on the eastern edge of the Philippine Sea plate. A *box* denotes the area of Fig. 45.1b. (**b**) A topographic map around 12°50′N. The *stars* represent the positions of hydrothermal fields in this study. *S*, *Y*, *A*, *P*, and *U* denote the initial letter of Snail, Yamanaka, Archaean, Pika, and Urashima sites, respectively

2011; Little et al. 2004; Kato et al. 2009; Langley et al. 2009; Toner et al. 2009). Ecosystems based on metabolism of inorganic materials are of interest for their potential insight into the origins of life (e.g., Alt 1988; Juniper and Fouquet 1988; Duhig et al. 1992; Juniper and Tebo 1995; Hofmann and Farmer 2000; Reysenbach and Cady 2001).

In the context of the TAIGA project, hydrothermal activity in the Southern Mariana Trough is recognized as Sulfur TAIGA and Iron TAIGA (Urabe et al. Chap. 1), and the project aims to elucidate what kind of ecosystems are prevalent, what kind of metabolisms they employ, and what kind of chemical environments they live in (Urabe et al. 2009). In this tectonic setting, in which hydrothermal activities are extending southward, how ecosystems propagate may shed light on more general questions about the evolution of life processes. Also, a fundamental question about mass flux at Earth's surface is the influence of subducting materials and magmatic volatiles. Extremely acidic fluids affected by magmatic volatiles raise the solubility of metals and mobilize them from rocks to fluids (Gamo et al. 1997b, 2006; Gena et al. 2001; Yang and Scott 2006). This aspect of the metal supply may have a great influence on Fe-utilizing ecosystems. It was with these topics in mind that we investigated the chemical and isotopic compositions of hydrothermal fluids in the Southern Mariana Trough.

45.2 Geological Setting

In the Mariana Trough, the Pacific plate subducts beneath the Philippine Sea plate, and the shape of the trough is convex to the east as a result of backarc spreading (Fig. 45.1a). Spreading activity started between 5 and 10 Ma (Hussong and Uyeda 1981; Karig 1971; Bibee et al. 1980; Eguchi 1984; Yamazaki and Stern 1997), and the northern part of the Mariana Trough represents the early stage of rifting of a backarc basin (Yamazaki et al. 1993). The central part of the Mariana Trough, from 16° to 20°N, represents the early stage of backarc basin spreading, and the volcanic arc and backarc are clearly distinguishable (e.g., Hart et al. 1972; Hawkins 1977; Fryer et al. 1981; Natland and Tarney 1981). The backarc is very close to the volcanic arc south of 16°N, and the spreading center of the backarc is ambiguous south of 12.5°N (Hawkins 1977; Smoot 1990). The hydrothermal fields in this study are located around 13°N. Five hydrothermal systems have been discovered around 13°N, which are aligned perpendicular to the axis (Fig. 45.1b). The Snail and Yamanaka sites are on the spreading axis, and the Archaean, Urashima, and Pika sites are off the axis. Around the area, hydrothermal activities have been documented in the TOTO caldera (Gamo et al. 2004), Forecast vent field (Johnson et al. 1993), and Alice Springs field (Craig et al. 1987; Gamo 1993; Gamo et al. 1997a). Descriptions of these hydrothermal systems are found in the InterRidge Vents Database (Beaulieu 2013).

45.2.1 Snail Site

Snail site is on the spreading axis (12°57.214′N, 143°37.147′E, depth: 2,860 m) (Fig. 45.1b), where hydrothermal fluids as hot as 248 °C were observed in 2003 (Wheat et al. 2003). However, most of the seafloor around the site is covered by snails exposed to low-temperature fluid around 100 °C, and covered by a yellow microbial mat and shimmering fluid below 100 °C (Wheat et al. 2003). The microbial mat may be composed of iron hydroxide and associated with Fe-oxidizing bacteria (Kato et al. 2010). In 2004 and 2010, the Benthic Multicoring System (BMS) penetrated several meters below the seafloor, and basalt was recovered (Urabe et al. 2004). In 2012, an ROV investigation found that hydrothermal fluid of 45 °C was discharging from the casing pipe that was placed in the BMS drilling hole in 2004 (NT12-24 Cruise Report).

45.2.2 Yamanaka Site

Yamanaka site is on a mound about 30 m high on the spreading axis (12°57.6′N, 143°36.7′E, depth: 2,830 m), 1 km northwest of Snail (Fig. 45.1b). Observations have documented many sea anemones and dead chimneys as well as shimmering fluid below 20 °C seeping from the rocky seafloor (Kakegawa et al. 2008). Magnetic mapping in 2009 showed strong magnetization here, suggesting that hydrothermal alteration is weak (Fujii et al. 2013). Based on these facts, Yamanaka has been considered to be past its peak of hydrothermal activity (Yoshikawa et al. 2012).

45.2.3 Archaean Site

Archaean site is on a sulfide mound ~100 m high that is 2 km from the spreading axis (12°56.35′N, 143°38.0′E, depth: 2,990 m) (Fig. 45.1b). The ROV *ROPOS*, during cruise TN167A in 2004, documented black smokers venting fluid at temperatures up to 343 °C (Ishibashi et al. 2004). The BMS drilling campaign in 2010 recovered basalt and andesite from the base of the mound (Nakamura et al., Appendix 3-A1).

45.2.4 Pika Site

Pika site is on a 75 m-high knoll, with two peaks 5 km from the spreading axis (12°55.1′N, 143°38.9′E, depth: 2,830 m) (Fig. 45.1b). The manned submersible *Shinkai 6500*, during

cruise YK03-09 in 2003, documented a black smoker venting high-temperature fluid up to 330 °C at the top of the western peak of the knoll and no hydrothermal activity on the eastern peak (Utsumi et al. 2004). In 2004 the BMS campaign recovered andesite from borehole APM03 (Kakegawa et al. 2008), which means drilling site No.3 of Archaean Park Project in Mariana (Urabe et al. 2001).

45.2.5 Urashima Site

Urashima site is on a mound several meters high 500 m north of Pika (12°55.30′N, 143°38.89′E, depth 2,922 m) (Fig. 45.1b), and several gray smokers venting hydrothermal fluids as hot as 280 °C were documented by *Shinkai 6500* during cruise YK10-10 in 2010 (Nakamura et al. 2013). A strong negative magnetic anomaly was observed by the autonomous underwater vehicle (AUV) *Urashima* in 2009 (Seama et al. Chap. 17), suggesting demagnetization by hydrothermal alteration (Rona 1978; Tivey and Johnson 2002). The site includes black dead chimneys, red-brown shimmering chimneys, and areas of yellow microbial mat exposed to low-temperature hydrothermal fluids. The microbial mat is probably composed of iron hydroxide like that at Snail.

45.3 Materials and Methods

45.3.1 Sampling Methods

Hydrothermal fluids were collected during YK03-09 (October, 2009), TN167A (March, 2004), YK05-09 (July, 2005), YK10-10 (August, 2010), YK10-13 (October, 2010), and NT12-24 (September, 2012) (Suppl. 45.1a and 45.1b) using the ROCS and the WHATS (Tsunogai et al. 2003; Saegusa et al. 2006). The WHATS is multi-bottle gastight sampling system, which avoids degassing and contamination by tightly closing the valves of sample bottles in situ. During sampling, the bottle inlet was held as close as possible to the hydrothermal vent, but in typical operation the inlet sometimes drops off the vent and draws in seawater. With allowance for a small degree of seawater admixture, the sample represents the average composition of hydrothermal fluid during the sampling period. The fluid temperature was recorded during sampling. The samples were collected with two bottles at each vent, one for gas analyses and the other for fluid analyses.

The sample for fluid analyses was first subsampled into two 5-mL vials for measurement of pH, alkalinity, and H_2S concentration. The remaining fluid was then filtered using a 0.45-μm pore-size disk filter attached to a plastic syringe and distributed into 15- and 30-mL plastic bottles. The 15-mL subsample was measured for NH_4^+ and Si concentrations on board, and Cl^- and SO_4^{2-} concentrations on land. The 30-mL subsample was combined with 300 μL of 3N HNO_3 on board the tender ship and then measured for major and minor elements on shore.

The sample bottle for gas analyses was processed as soon as possible (Konno et al. 2006); the fluid in the bottle was transferred to a 300-mL evacuated glass container, then acidified with amidosulfuric acid to convert all dissolved carbonate species to CO_2 in the headspace of the container. The fluid was treated with sufficient $HgCl_2$ to thoroughly convert H_2S to HgS in the vacuum line. The gas phase was transferred to a 50-mL evacuated stainless steel container for gas analyses on shore, and then the residual fluid in the container was filtered for measurement of major elements on shore.

45.3.2 Analysis

The pH was measured by electrode with a precision of ±0.02 (Gieskes et al. 1991). The calibration was done using buffers of pH 4.01 and pH 6.86 once a day before the measurements. Alkalinity was measured by HCl titration, which endpoint was determined by the Gran's plot, with a precision of ±2 % (Gieskes et al. 1991). The concentration of H_2S was measured by colorimetry using methylene blue with a precision of ±10 %. Ammonia concentration was measured by colorimetry using phenol blue with a precision of ±8 %. The Si concentration was determined by colorimetry using molybdate blue with a precision of ±1 %. Chlorinity was analyzed by the Mohr method with a precision of ±1 %. The SO_4^{2-} concentration was determined by ion chromatography with a precision of ±4 %. Major and minor elements (Na, Ca, Mg, Sr, Ba, Mn, Fe, Si, B, and Li) were analyzed by inductively coupled plasma atomic emission spectroscopy (ICP-AES). The K concentration was analyzed by atomic absorption spectrometry. The Na concentration was also calculated independently on the basis of charge balance.

Gas concentrations of O_2, N_2, CO_2, H_2, and He were measured by using gas chromatography with a thermal conductivity detector. CH_4 concentration and its stable carbon isotope ratio were determined with a continuous-flow isotope ratio mass spectrometer (CF-irMS) (Tsunogai et al. 2000). The hydrogen isotope ratio (D/H) of CH_4 was analyzed by using a CF-irMS with a precision of ±10 ‰. The hydrogen isotope ratio of H_2 was analyzed by using a CF-irMS with a precision of ±4 ‰ (Komatsu et al. 2011). Helium isotope ratios ($^3He/^4He$) were measured by using noble gas mass spectrometry with a precision of ±2 % (Sano et al. 2006). The ratio of ^4He to ^{20}Ne was determined by using quadrupole mass spectrometry with a precision of ±10 % (Sano et al. 2006). Dissolved organic matter was measured with a Shimadzu TOC-5000 total organic carbon analyzer with a high-temperature catalytic method.

45.4 Results

The analytical results for hydrothermal fluids from the five sites are shown in Suppl. 45.1a for fluid chemistry and Suppl. 45.1b for gas chemistry, together with the maximum and average temperatures recorded during sampling.

45.4.1 Calculation of End-Member Compositions

Graphs of the concentrations of each chemical component relative to Mg concentration are shown in Fig. 45.2. Under the assumption that pure hydrothermal fluid is free of Mg, its chemical composition was calculated as the y-axis intercept of linear relationship among data plots (Von Damm 1995). The Yamanaka site yielded only low-temperature hydrothermal fluids with compositions that could not be distinguished from that of seawater, and this site is not discussed further. End-member concentrations of the hydrothermal fluids in the remaining four sites are listed in Table 45.1 for aqueous components and Table 45.2 for volatile components, and discussed below.

The end-member carbon isotopic composition of methane, $\delta^{13}C(CH_4)$, was estimated as the intercept of the y-axis on a graph of $\delta^{13}C(CH_4)$ against the reciprocal of CH_4 concentration, as shown in Fig. 45.3 (Keeling 1961). Estimates of this type are based on the assumption that the background concentration is negligible. In the case of methane, background CH_4 in seawater is several nM, whereas CH_4 in hydrothermal fluid is several hundred μM, a difference of five orders of magnitude.

However, because the background CO_2 concentration is substantial in seawater (2 mM) compared to hydrothermal fluid (several tens mM), we relied on a method used in atmospheric chemistry to evaluate end-member $\delta^{13}C(CO_2)$ (Miller and Tans 2003). As illustrated in Fig. 45.4, a product that CO_2 concentration multiplies $\delta^{13}C(CO_2)$ is plotted to CO_2 concentration, when the slope can be taken as $\delta^{13}C(CO_2)$ of the source.

Helium in hydrothermal gases is a mixture of mantle, crust, and seawater contributions. Because ^{20}Ne is negligible in rock, helium isotope ratios can be corrected for seawater admixture using $^4He/^{20}Ne$ ratios, as shown in Fig. 45.5 (Craig et al. 1978).

45.4.2 End-Member Concentrations of Dissolved Constituents

Maximum fluid temperatures were as follows: Snail, 116 °C; Archaean, 343 °C; Pika, 330 °C; Urashima, 280 °C (Table 45.1).

The lowest pH ranged from 2.8 to 3.5, and only at Snail was it greater than 3. Except for Snail, these values are lower than that of hydrothermal fluids in mid-ocean ridges ranging about 3–3.5 on average (Von Damm 1995).

The end-members for all sites have negative alkalinity; −0.94 for Snail, −1.41 for Archaean, −1.14 for Pika, and −1.44 for Urashima. These data suggests that these hydrothermal fluids have substantial strong acidity compared with hydrothermal fluid in the mid-ocean ridge setting, where the fluid is rather neutralized during high temperature fluid-rock interactions. This view is supported by relatively low pH in Southern Mariana Trough hydrothermal fluids.

The Si concentrations were measured by colorimetry on board and by ICP-AES on land, and both end-member concentrations were consistent with each other. Values lay in a narrow range between 16.4 and 17.0 mM except for Snail, where the Si concentration was greater than 18 mM.

The end-member Cl^- concentrations deviated from that of seawater (550 mM) at all sites. At Archaean, the Cl^- end-member in 2004 (466 mM) had a higher concentration than those in 2005 and 2010 (407 mM). At Pika, high-Cl^- fluids (603 mM) were consistently reported after its discovery in 2003, but a low-Cl^- fluid (460 mM) was recovered in 2010 (Table 45.1). Such Cl^- deviations from that of seawater have been reported in many hydrothermal systems in the world, which are thought to be due to phase separation beneath the seafloor (Von Damm 1995). Especially, higher-Cl^- and lower-Cl^- fluids than that of seawater have been sampled, like those at Pika, suggesting that active phase separation beneath the seafloor has occurred there, as mentioned in many hydrothermal systems in the world (Von Damm 1995). A positive Cl^- deviation from that of seawater, like those at Urashima, can be due to input of HCl derived from magmatic volatiles, as mentioned at DESMOS hydrothermal field in Manus Basin (Gamo et al. 1997b). In that case, the hydrothermal fluids also have extremely low pH and an excess of SO_4^{2-} (Gamo et al. 1997b), and we found that hydrothermal fluids from Urashima site have an end-member pH slightly lower than 3 as mentioned above (Table 45.1).

The Na concentration was independently calculated by charge balance as well as measured by ICP-AES. The calculated values were more clearly linear relative to Mg concentrations than the measured values. Although the errors of the calculated concentrations are larger than those of the measured concentrations, we took the calculated values as those of the preferred end-members. The end-member value for Snail was close to that of seawater (460 mM). The end-member Na concentration for Archaean (345 mM) was lower than that of seawater. At Pika, the end-member value in 2003 and 2005 was higher than that of seawater, although sample D1219 W-4, taken in 2010, had a lower value than seawater (Table 45.1). For Urashima, the

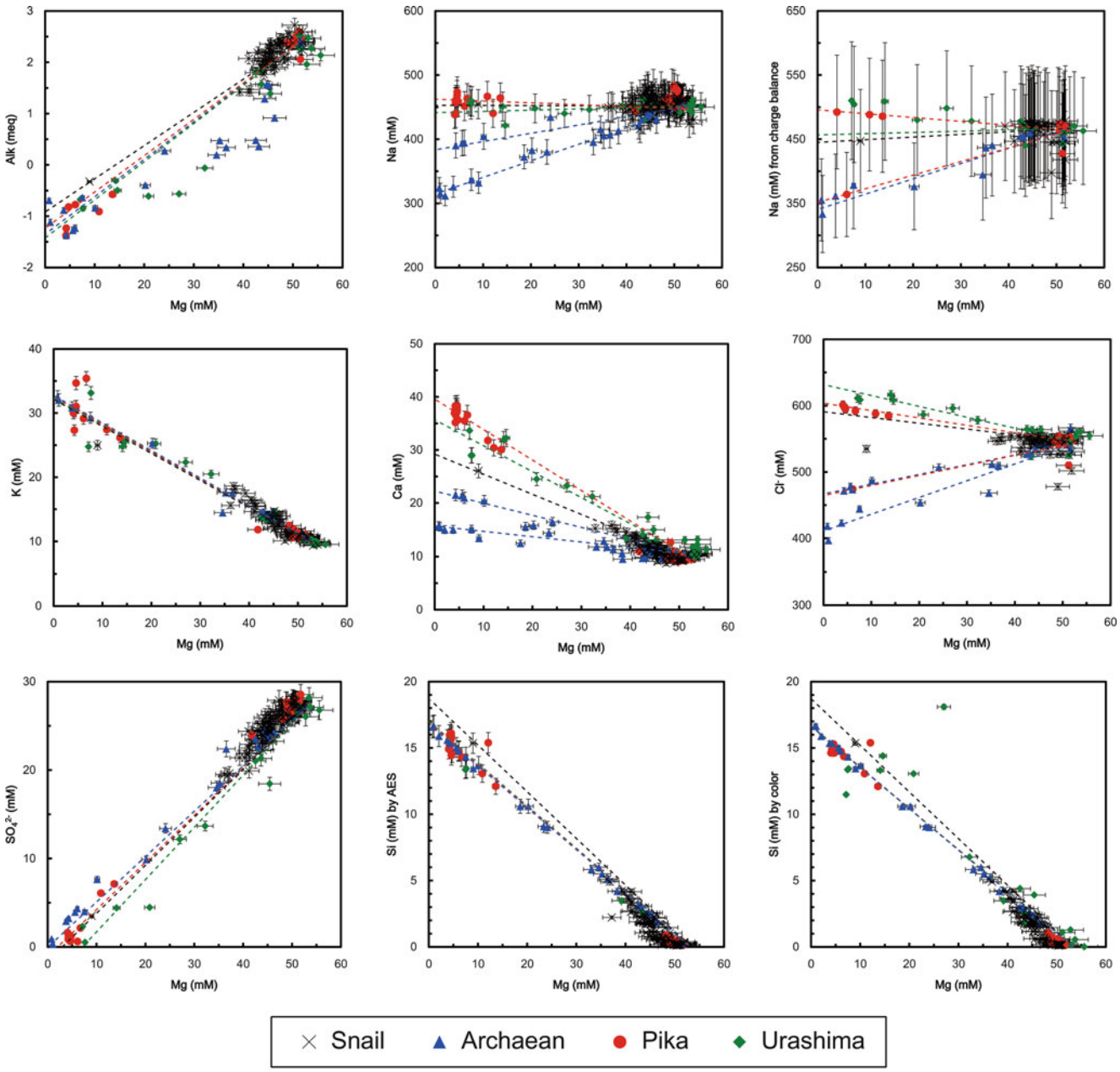

Fig. 45.2 A plot of each chemical component vs. Mg concentration in the hydrothermal fluid for each site in the Southern Mariana Trough in this study

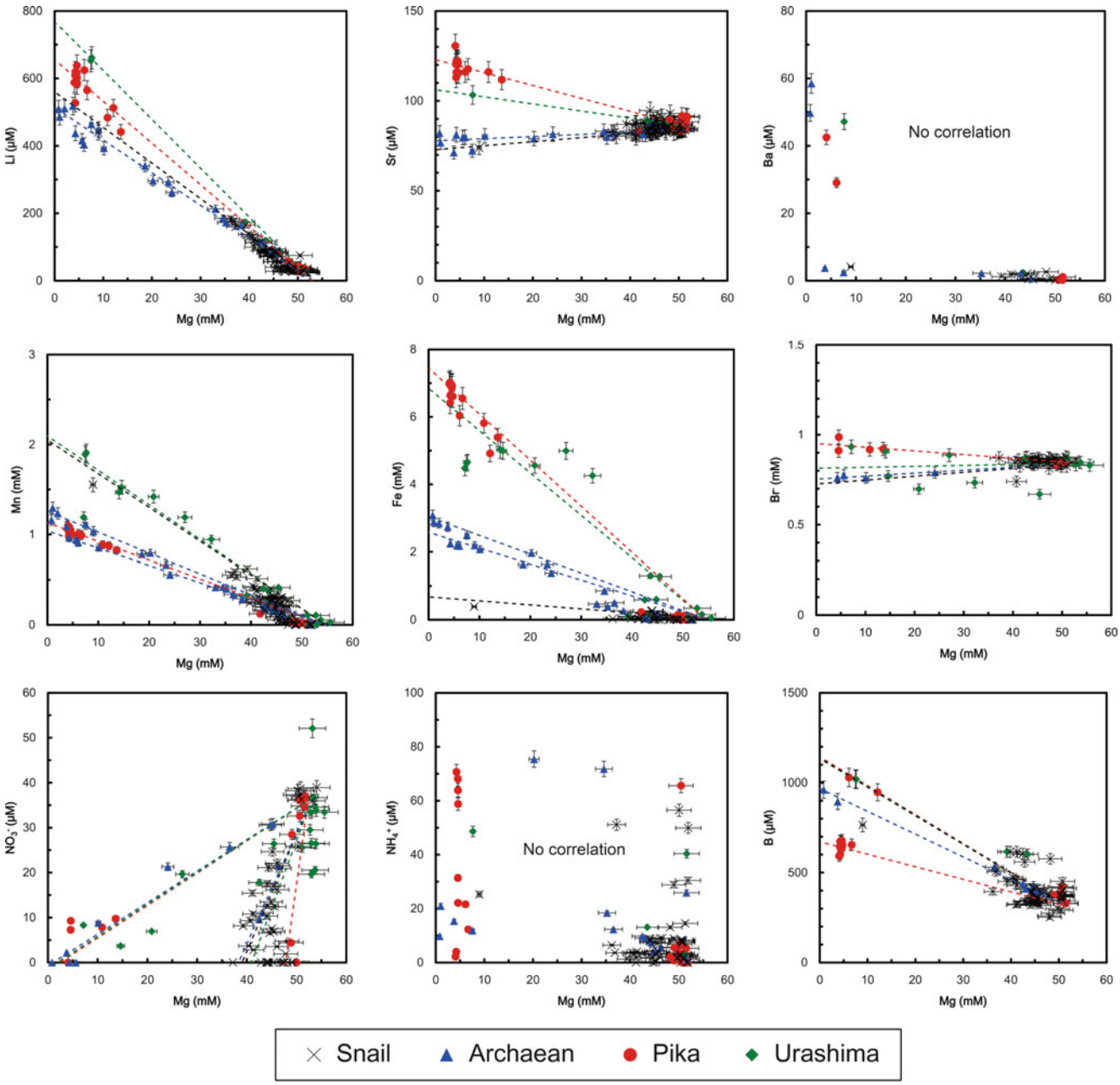

Fig. 45.2 (continued)

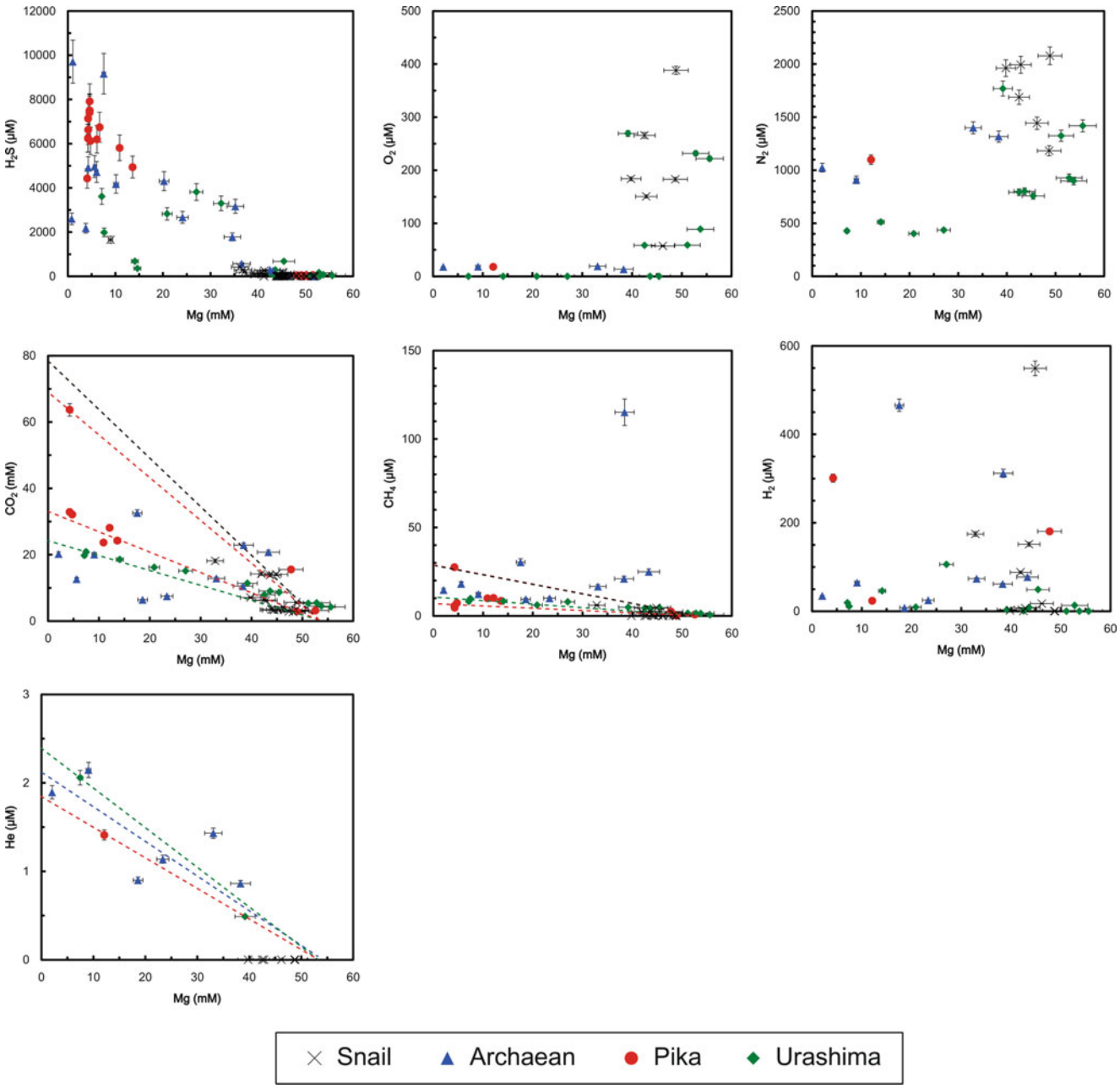

Fig. 45.2 (continued)

end-member Na concentration (515 mM) was higher than that of seawater.

For Ca concentrations, the end-members for all four sites had higher values than that of seawater (10 mM). At Archaean, the end-member Ca concentration for 2004 was higher than the one for 2005 and 2010, which is similar to our finding for Cl^- concentrations.

For K concentrations, end-member values for all sites fell into a narrow range (31.3–32.8 mM), and the values for Pika and Archaean were significantly higher than those for Snail and Urashima.

For Fe concentrations, the end-members for all four sites had higher concentrations than that of seawater (<1 nM). The end-member value was 0.64 mM for Snail, 2.55 mM for Archaean in 2003–2005, 3.00 mM for Archaean in 2010, 7.38 mM for Pika, and 6.37 mM for Urashima (Table 45.1). The end-member Fe concentration at Snail site is as low or lower when compared to those in the

hydrothermal fluids in EPR21°N (0.2–2.4 mM; Von Damm et al. 2002), but otherwise those in the Southern Mariana Trough appear higher as compared with those in EPR21°N. Fe leaches from rocks at low pH attributed to an input of magmatic volatiles (Mottl et al. 1979; Hajash and Chandler 1982; Seyfried and Janecky 1985; Seewald and Seyfried 1990). The cause of Fe enrichment in Pika, Urashima, and Archaean sites would be low pH coming from an input of magmatic volatiles.

The end-members of major elements had two concentrations for both Pika and Archaean and unique values for both Snail and Urashima (Table 45.1).

45.4.3 Distribution of Gas Components

Dissolved oxygen concentrations showed nonlinear relationships to Mg concentrations, so end-member concentrations were not computed (Fig. 45.2). We just explain the concentration for each Mg concentration (Suppl. 45.1b and Fig. 45.2). At Snail, samples contained Mg concentrations higher than 40 mM and had oxygen concentrations higher than that of seawater, ranging around 100–200 μM. At Archaean, samples had Mg concentrations lower than 40 mM and oxygen concentrations lower than 20 μM. The single sample from Pika contained 12 mM Mg and an oxygen concentration of 18 μM. Urashima yielded samples containing from 7 to 54 mM Mg, and oxygen was not detected in samples with less than 40 mM Mg.

Dissolved nitrogen was detected in all samples, but its concentrations showed nonlinear relationships to Mg concentrations (Fig. 45.2). At Snail, all samples contained Mg concentrations above 40 mM, and nitrogen concentrations were higher than that of seawater (500–1,000 μM). At Archaean, two samples had Mg concentrations around 10 and 30 mM, and the N_2 concentration of the latter was higher than that of the former. The single sample from Pika had a Mg concentration of 12 mM and a N_2 concentration of about 1 mM.

End-member dissolved CO_2 concentrations were calculated for each site from their relation to Mg concentrations (data for Archaean did not fit a linear relation). The end-member values were all higher than that of seawater (2.4 mM). At Snail, although the majority of samples had values close to that of seawater, the end-member value, 78.8 mM, was highest among our sites. Although we did not calculate an end-member concentration for Archaean, the range of CO_2 concentrations there was 6.4–32.6 mM. For Pika, samples taken in 2005 had an especially high value (69.1 mM); whereas the end-member concentration for 2003, 2004, and 2010 samples was much lower (33.7 mM). For Urashima, the end-member value was 23.2 mM. The reported range of CO_2 concentrations in hydrothermal fluids from EPR are lower than 10 mM (Von Damm et al. 2002), and so the observed CO_2 concentrations in hydrothermal fluids in the Southern Mariana Trough in this study are relatively higher than those in EPR. Such CO_2 enrichments could be influenced by a little input of magmatic volatiles, as mentioned in hydrothermal systems related to arc systems (Sakai et al. 1990; Gamo 1993; Tsunogai et al. 1994; Gamo et al. 2006; Lupton et al. 2008).

The end-member value of CH_4 for Snail was 29.6 μM, although the error was large because values for most samples were close to seawater values. For Archaean, the data were too scattered to calculate an end-member concentration, but sample D903 W-3, from a clear smoker vent with a maximum temperature of 117 °C, had the highest concentration of CH_4 in this study, 115 μM. For Pika, the 2005 end-member concentration (29.9 μM) was higher than the end-member concentration for the other years (7.2 μM). The end-member value for Urashima was 10.8 μM.

Hydrogen concentrations were not linearly related to Mg concentrations, and we did not calculate H_2 end-member concentrations. The maximum H_2 concentrations were 549 μM at Snail, 466 μM at Archaean, 301 μM at Pika and 105 μM at Urashima.

Helium was not detected in Snail samples. For Archaean, the relation of He to Mg concentrations was not clearly linear, but the end-member concentration was calculated to be 2.1 μM. Although we have only one sample from Pika, the end-member value was 1.8 μM. For Urashima, given the helium concentration in seawater (2 nM), the relationship between He and Mg concentrations was smoothly linear, and the end-member value was 2.4 μM.

45.4.4 Isotopic Compositions of End-Members

The end-member $\delta^{13}C(CO_2)$ ranged from −2.3 to +0.1 ‰ (all values are relative to VPDB): −1.3 ‰ for Snail, −2.0 ‰ for Archaean, +0.1 ‰ for Pika, and −2.4 ‰ for Urashima (Table 45.2), which was the only value higher than that of seawater (0 ‰).

The $\delta^{13}C(CH_4)$ values showed a nonlinear relationship to $1/CH_4$. For Snail, the $\delta^{13}C(CH_4)$ values in CH_4-rich samples were around −5 ‰ and −25 ‰ for Snail, −10 ‰ and −50 ‰ for Archaean, around −5 ‰ for Pika, and −5 ‰ and −0 ‰ for Urashima.

The helium isotope ratios in source fluids, corrected for seawater admixture, were $8.1R_A$ for Snail, $8.4R_A$ for Archaean, $8.3R_A$ for Pika, and $8.0R_A$ for Urashima.

Table 45.1 End-member concentrations of aqueous components in the hydrothermal fluids for all the sites in the Southern Mariana Trough in this study

							CB									
Site	T_{max}	pH_{min}	Alk. (meq)	ΔAlk (meq)	Na (mM)	ΔNa (mM)	Na (mM)	ΔNa (mM)	K (mM)	ΔK (mM)	Li (μM)	ΔLi (μM)	Ca (mM)	ΔCa (mM)	Sr (μM)	ΔSr (μM)	Ba (μM)
Snail	116	3.52	−0.94	±0.04	454	±21	466	±91	31.3	±0.7	555	±22	29.9	±1.1	71.9	±4.0	N.D.
Archaean	343	2.94	−1.41	±0.03					32.8	±0.5	500	±8			76.6	±1.5	N.D.
2004					388	±11							20.6	±0.5			
2005–2010					315	±7	345	±33					15.7	±0.3			
Pika	330	2.86	−1.14	±0.02					32.6	±0.3	644	±9	39.4	±0.5	122.8	±1.7	N.D.
2003–2005					461	±7	495	±63									
2010					436	±15	351	±75									
Urashima	280	2.85	−1.44	±0.03	447	±11	515	±56	31.7	±0.5	764	±28	35.2	±0.8	106.2	±6.3	N.D.

CB means the Na concentrations are calculated by charge balance
AES and Color means the Si concentration are measured by ICP-AES and colorimetry, respectively

Table 45.2 End-member compositions of volatile components in the hydrothermal fluids for all the sites in the Southern Mariana Trough in this study

Site	T_{max}	H_2S (μM)	ΔH_2S (μM)	O_2 (μM)	N_2 (μM)	CO_2 (mM)	ΔCO_2 (mM)	CH_4 (μM)	ΔCH_4 (μM)	H_2 (μM)
Snail	116			N.D.	N.D.	78.8	±12.4	29.6	±5.1	N.D.
Archaean	343			N.D.	N.D.	N.D.	N.D.	N.D.	N.D.	N.D.
2004										
2005–2010										
Pika	330			N.D.	N.D.	33.7	±0.6	7.2	±0.2	N.D.
2005						69.1	±2.1	29.9	±2.0	
Urashima	280	883	±43	N.D.	N.D.	23.2	±0.4	10.8	±0.3	N.D.

N.D. not determined

													AES		Color			
Mn (mM)	ΔMn (mM)	Fe (mM)	ΔFe (mM)	Cl (mM)	ΔCl (mM)	SO_4 (mM)	ΔSO_4 (mM)	Br (mM)	ΔBr (mM)	NO_3 (μM)	ΔNO_3 (μM)	NH_4 (μM)	Si (mM)	ΔSi (mM)	Si (mM)	ΔSi (mM)	B (μM)	ΔB (μM)
2.08	±0.08	0.64	±0.02	588	±6	−1.71	±0.37	0.72	±0.10	−269	±53	N.D.	18.6	±0.8	18.7	±0.3	1,112	±37
						0.01	±0.03	0.75	±0.02			N.D.	16.7	±0.3	16.7	±0.1	959	±34
1.06	±0.02	2.55	±0.06	466	±3					−0.82	±0.04							
1.2	±0.02	3.00	±0.06	407	±2					−372	±5,609							
1.13	±0.01	7.38	±0.10			−1.57	±0.06	0.95	±0.02			N.D.	16.9	±0.2	16.4	±0.1		
				603	±3					−992	±3,483						1,130	±43
				460	±5					−1.5	±0.2						673	±10
2.22	±0.08	6.37	±0.13	629	±4	−3.02	±0.20	0.81	±0.02	−0.9	±0.3	N.D.	17.0	±0.4	16.5	±0.1	1,109	±45

He (μM)	ΔHe (μM)	$\delta^{13}C(CO_2)$ (‰VPDB)	$\Delta\delta^{13}C(CO_2)$ (‰VPDB)	$\delta^{13}C(CH_4)$ (‰VPDB)	$\delta D(H_2)$ (‰VSMOW)	$\delta D(CH_4)$ (‰VSMOW)	$^3He/^4He$ (R_A)	$\Delta^3He/^4He$ (R_A)
N.D.	N.D.	−1.33	±0.10	N.D.	N.D.	N.D.	8.15	±0.09
2.10		−2.00	±0.61	N.D.	N.D.	N.D.	8.37	±0.03
1.83	±0.08	0.14	±0.06	N.D.	N.D.	N.D.	8.27	±0.10
2.40	±0.1	−2.36	±0.17	N.D.	N.D.	N.D.	8.09	±0.19

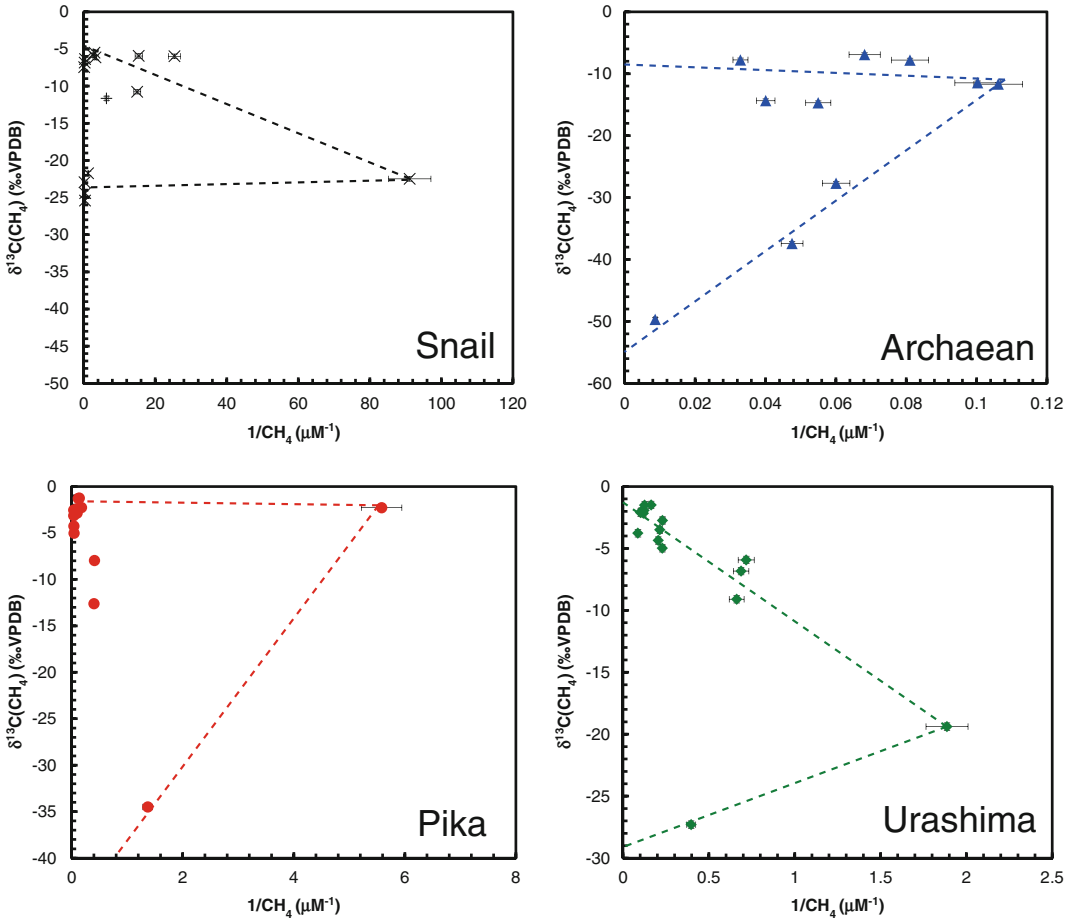

Fig. 45.3 Plots of $\delta^{13}C$ vs. 1/(CH_4 concentration) in the hydrothermal fluids for all the sites in the Southern Mariana Trough in this study

45.5 Summary

Hydrothermal fluids were sampled from several hydrothermal activities around the Southern Mariana backarc spreading center, and analyzed for chemical and isotopic compositions. The fluid chemistry around the Southern Mariana Trough would be influenced by a little input of magmatic volatiles, leading to low pH and high CO_2 concentrations, consequently the hydrothermal fluids are characterized by rich in Fe alongside of the MOR hydrothermal fluids.

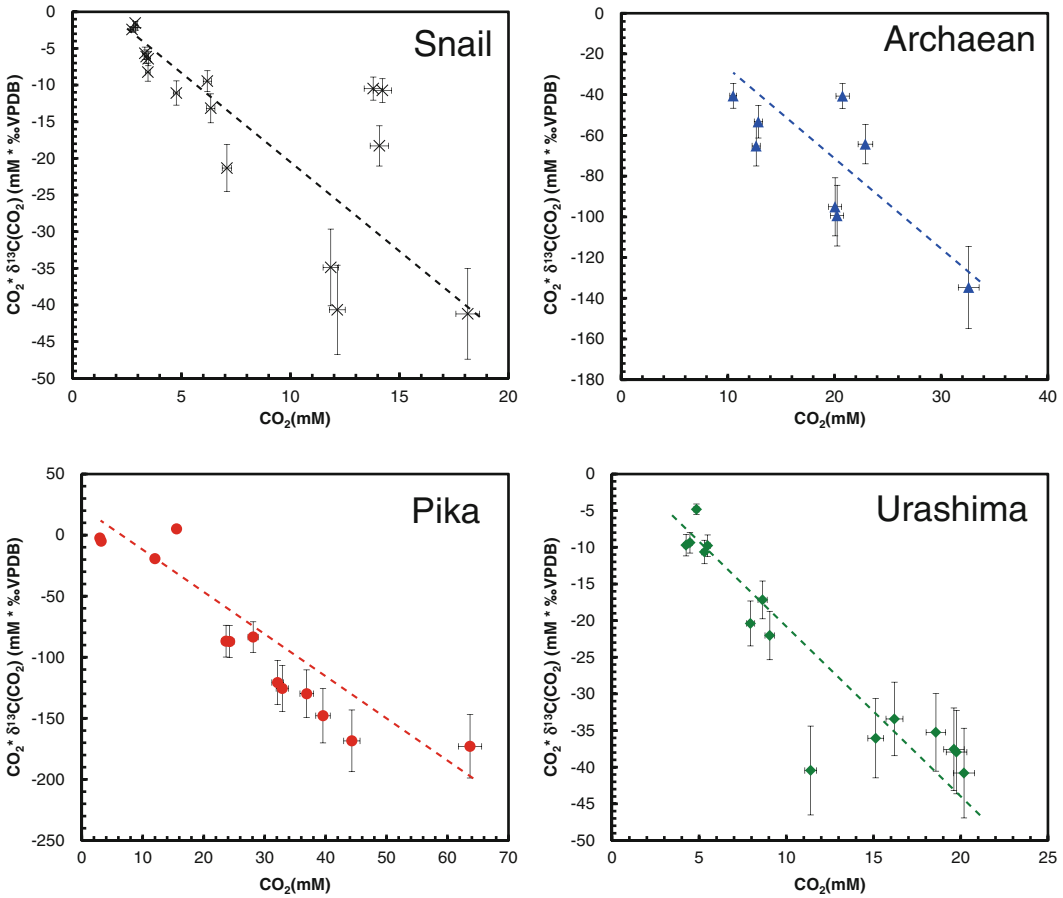

Fig. 45.4 Relationship between CO_2 concentrations and isotopic index from all the sites in the Southern Mariana Trough in this study are plotted, where the index are calculated by multiplying $\delta^{13}C(CO_2)$ by CO_2 concentrations

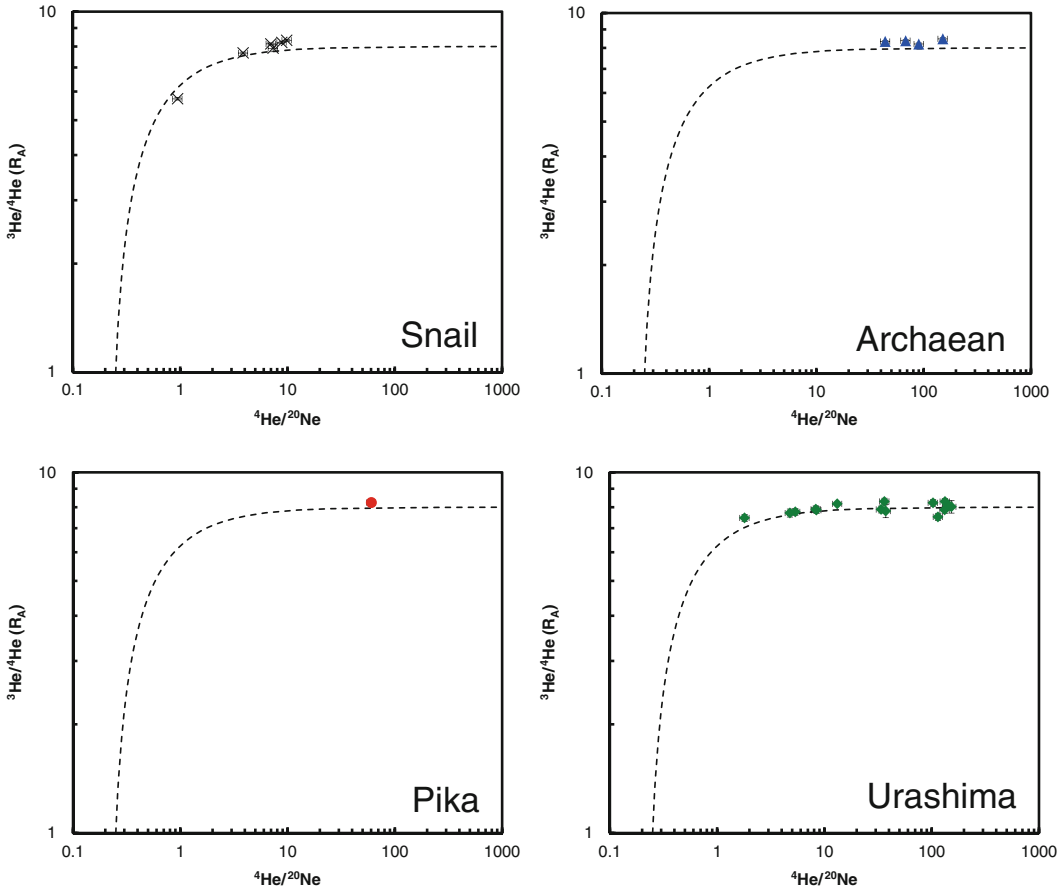

Fig. 45.5 Relationship between $^4He/^{20}Ne$ and $^3He/^4He$ in the hydrothermal fluids for all the sites in the Southern Mariana Trough in this study, together with the mixing line between mantle and seawater

Acknowledgments We thank the captains and crews of the *Yokosuka* and *Natsushima* and the commanders and operation teams of the *Shinkai 6500* and Hyper-Dolphin for sampling. Constructive and helpful reviews by Dr. Shinsuke Kawagucci and Dr. Takezo Shibuya are gratefully acknowledged. This study was supported by the Grant-in-Aid for Scientific Research on Innovative Areas of the Ministry of Education, Culture, Science and Technology (MEXT) "TAIGA project (Trans-crustal Advection and In situ biogeochemical processes of Global sub-seafloor Aquifer)," and partly by International Research Hub Project for Climate Change and Coral Reef/Island Dynamics from the University of the Ryukyus.

References

Alt JC (1988) Hydrothermal oxide and nontronite deposits on seamounts in the eastern Pacific. Mar Geol 81(1–4):227–239

Beaulieu SE (2013) InterRidge global database of active submarine hydrothermal vent fields, InterRidge

Bibee LD, Shor GG Jr, Lu RS (1980) Inter-arc spreading in the Mariana Trough. Mar Geol 35(1–3):183–197

Boyd TD, Scott SD (2001) Microbial and hydrothermal aspects of ferric oxyhydroxides and ferrosic hydroxides: the example of Franklin Seamount, Western Woodlark Basin, Papua New Guinea. Geochem Trans 2:45

Craig H, Lupton JE, Horibe Y (1978) A mantle helium component in circum-pacific volcanic gases: Hakone, the Marianas, and Mt. Lassen. In: Alexander EC, Ozima M (eds) Terrestrial rare gases. Japan Science Society Press, Tokyo, pp 3–16

Craig H, Horibe Y, Farley KA (1987) Hydrothermal vents in the Mariana Trough: results of the first Alvin dives. Eos Trans AGU 68(44):1531

Deming JW, Baross JA (1993) Deep-sea smokers: windows to a subsurface biosphere? Geochim Cosmochim Acta 57(14):3219–3230

Duhig NC, Davidson GJ, Stolz J (1992) Microbial involvement in the formation of Cambrian sea-floor silica-iron oxide deposits, Australia. Geology 20(6):511–514

Edwards KJ (2004) Formation and degradation of seafloor hydrothermal sulfide deposits. Geolog Soc Am Spec Paper 379:83–96

Edwards KJ, McCollom TM, Konishi H, Buseck PR (2003) Seafloor bioalteration of sulfide minerals: results from in situ incubation studies. Geochim Cosmochim Acta 67(15):2843–2856

Edwards KJ et al (2011) Ultra-diffuse hydrothermal venting supports Fe-oxidizing bacteria and massive umber deposition at 5000 m off Hawaii. ISME J 5(11):1748–1758

Eguchi T (1984) Seismotectonics around the Mariana trough. Tectonophysics 102(1–4):33–52

Fryer P (1995) Geology of the Mariana Trough. In: Taylor B (ed) Backarc basins tectonics and magmatism. Plenum, New York, pp 237–279

Fryer P, Sinton JM, Philpotts JA (1981) Basaltic glasses from the Mariana Trough. In: Hussong DM, Uyeda S, Knapp R, Ellis H, Kling S, Natland J (eds) Initial reports of the deep sea drilling project. U.S. Government Printing Office, Washington DC, pp 601–610

Fujii M, Okino K, Honsho C, Dyment J, Florent S, Mochizuki N (2013) Developing near-bottom magnetic measurements using a 3D forward modeling technique: application to hydrothermal vent fields, paper presented at Underwater Technology Symposium (UT), 2013 IEEE International, pp 5–8 March 2013

Gamo T (1993) Revisits to the mid-Mariana Trough hydrothermal site and discovery of new venting in the southern Mariana region by the Japanese submersible Shinkai 6500. InterRidge News 2:11–14

Gamo T, Tsunogai U, Ishibashi J, Masuda H, Chiba H (1997a) Chemical characteristics of hydrothermal fluids from the Mariana Trough. JAMSTEC J Deep Sea Res 69–74 (Special volume, Deep Sea Research in subduction zones, spreading centers and backarc basins, JAMSTEC)

Gamo T, Okamura K, Charlou J-L, Urabe T, Auzende J-M, Ishibashi J, Shitashima K, Chiba H, Shipboard Scientific Party of the Manus Flux Cruise (1997b) Acidic and sulfate-rich hydrothermal fluids from the Manus back-arc basin, Papua New Guinea. Geology 25 (2):139–142

Gamo T et al (2004) Discovery of a new hydrothermal venting site in the southernmost Mariana Arc: Al-rich hydrothermal plumes and white smoker activity associated with biogenic methane. Geochem J 38(6):527–534

Gamo T, Ishibashi J, Tsunogai U, Okamura K, Chiba H (2006) Unique geochemistry of submarine hydrothermal fluids from arc-back-arc settings of the western Pacific. In: Ridge 2000-InterRidge Theoretical Institute "interactions among physical, chemical, biological, and geological processes in backarc spreading systems". American Geophysical Union, Washington DC, pp. 147–161

Gena K, Mizuta T, Ishiyama D, Urabe T (2001) Acid-sulphate type alteration and mineralization in the Desmos caldera, Manus back-arc basin, Papua New Guinea. Resour Geol 51(1):31–44

Gieskes JM, Gamo T, Brumsack H (1991) Chemical methods for interstitial water analysis aboard JOIDES Resolution. Ocean Drill Prog Texas A&M Univ Tech Note 15:1–60

Hajash A, Chandler G (1982) An experimental investigation of high-temperature interactions between seawater and rhyolite, andesite, basalt and peridotite. Contr Mineral Petrol 78(3):240–254

Hart SR, Glassley WE, Karig DE (1972) Basalts and sea floor spreading behind the Mariana Island arc. Earth Planet Sci Lett 15(1):12–18

Hawkins JW Jr (1977) Petrologic and geochemical characteristics of marginal basin basalts. In: Hayes DE (ed) Island arcs, deep sea trenches and backarc basins. AGU, Washington DC, pp 355–365

Hofmann BA, Farmer JD (2000) Filamentous fabrics in low-temperature mineral assemblages: are they fossil biomarkers? Implications for the search for a subsurface fossil record on the early Earth and Mars. Planet Space Sci 48(11):1077–1086

Hussong DM, Uyeda S (1981) Tectonic processes and the history of the Mariana Arc, a synthesis of the results of deep sea drilling project Leg 60. In: Hussong DM, Uyeda S, Knapp R, Ellis H, Kling S, Natland J (eds) Initial reports of the deep sea drilling project. U.S. Government Printing Office, Washington DC, pp 909–929

Ishibashi J et al (2004) Geochemistry of hydrothermal fluids in south Mariana backarc spreading center, paper presented at AGU Fall Meeting 2004. American Geophysical Union, San Francisco, V44A-05

Johnson LE, Fryer P, Masuda H, Ishii T, Gamo T (1993) Hydrothermal deposits and two magma sources for volcanoes near 13°20′N in the Mariana backarc: a view from Shinkai 6500. EOS Trans AGU Fall Meet Suppl 74(43):681

Juniper SK, Fouquet Y (1988) Filamentous iron-silica deposits from modern and ancient hydrothermal sites. Can Mineral 26(3):859–869

Juniper SK, Tebo BM (1995) Microbe-metal interactions and mineral deposition at hydrothermal vents. In: Karl DM (ed) The microbiology of deep-sea hydrothermal vents. CRC Press, Boca Raton, pp 219–253

Kakegawa T, Utsumi M, Marumo K (2008) Geochemistry of sulfide chimneys and basement pillow lavas at the Southern Mariana Trough (12.55°N–12.58°N). Resour Geol 58(3):249–266

Karig DE (1971) Structural history of the Mariana island arc system. Geol Soc Am Bull 82(2):323–344

Kato S, Kobayashi C, Kakegawa T, Yamagishi A (2009) Microbial communities in iron-silica-rich microbial mats at deep-sea hydrothermal fields of the Southern Mariana Trough. Environ Microbiol 11(8):2094–2111

Kato S et al (2010) Biogeography and biodiversity in sulfide structures of active and inactive vents at deep-sea hydrothermal fields of the Southern Mariana Trough. Appl Environ Microbiol 76 (9):2968–2979

Keeling CD (1961) The concentration and isotopic abundances of carbon dioxide in rural and marine air. Geochim Cosmochim Acta 24(3–4):277–298

Kelley DS, Baross JA, Delaney JR (2002) Volcanoes, fluids, and life at mid-ocean ridge spreading centers. Annu Rev Earth Planet Sci 30:385–491

Komatsu DD, Tsunogai U, Kamimura K, Konno U, Ishimura T, Nakagawa F (2011) Stable hydrogen isotopic analysis of nanomolar molecular hydrogen by automatic multi-step gas chromatographic separation. Rapid Commun Mass Spectrom 25(21):3351–3359

Konno U, Tsunogai U, Nakagawa F, Nakaseama M, Ishibashi J, Nunoura T, Nakamura K (2006) Liquid CO_2 venting on seafloor: Yonaguni IV Knoll hydrothermal system, Okinawa Trough. Geophys Res Lett 33, L16607

Langley S, Igric P, Takahashi Y, Sakai Y, Fortin D, Hannington MD, Schwarz-Schampera U (2009) Preliminary characterization and biological reduction of putative biogenic iron oxides (BIOS) from the Tonga-Kermadec Arc, southwest Pacific Ocean. Geobiology 7 (1):35–49

Little CTS, Glynn SEJ, Mills RA (2004) Four-hundred-and-ninety-million-year record of bacteriogenic iron oxide precipitation at sea-floor hydrothermal vents. Geomicrobiol J 21(6):415–429

Lupton J, Lilley M, Butterfield D, Evans L, Embley R, Massoth G, Christenson B, Nakamura K, Schmidt M (2008) Venting of a separate CO_2-rich gas phase from submarine arc volcanoes: examples from the Mariana and Tonga-Kermadec arcs. J Geophys Res Solid Earth 113(B8):B08S12

Miller JB, Tans PP (2003) Calculating isotopic fractionation from atmospheric measurements at various scales. Tellus B 55(2):207–214

Mottl MJ, Holland HD, Corr RF (1979) Chemical exchange during hydrothermal alteration of basalt by seawater—II. Experimental results for Fe, Mn, and sulfur species. Geochim Cosmochim Acta 43(6):869–884

Nakamura K, Toki T, Mochizuki N, Asada M, Ishibashi J, Nogi Y, Yoshikawa S, Miyazaki J, Okino K (2013) Discovery of a new hydrothermal vent based on an underwater, high-resolution geophysical survey. Deep Sea Res I 74:1–10

Natland JH, Tarney J (1981) Petrologic evolution of the Mariana arc and backarc basin system – a synthesis of drilling results in the south Philippine Sea. In: Hussong DM, Uyeda S et al (eds) Initial reports of the deep sea drilling project. U.S. Government Printing Office, Washington DC, pp 877–907

Reysenbach A-L, Cady SL (2001) Microbiology of ancient and modern hydrothermal systems. Trends Microbiol 9(2):79–86

Rona PA (1978) Magnetic signatures of hydrothermal alteration and volcanogenic mineral deposits in oceanic crust. J Volcanol Geotherm Res 3(1–2):219–225

Saegusa S, Tsunogai U, Nakagawa F, Kaneko S (2006) Development of a multibottle gas-tight fluid sampler WHATS II for Japanese submersibles/ROVs. Geofluids 6(3):234–240

Sakai H, Gamo T, Kim ES, Tsutsumi M, Tanaka T, Ishibashi J, Wakita H, Yamano M, Oomori T (1990) Venting of carbon dioxide-rich fluid and hydrate formation in mid-Okinawa Trough backarc basin. Science 248(4959):1093–1096

Sano Y, Takahata N, Seno T (2006) Geographical distribution of $^{3}He/^{4}He$ ratios in the Chugoku district, southwestern Japan. Pure Appl Geophys 163(4):745–757

Seewald JS, Seyfried WE Jr (1990) The effect of temperature on metal mobility in subseafloor hydrothermal systems: constraints from basalt alteration experiments. Earth Planet Sci Lett 101(2–4):388–403

Seyfried WE Jr, Janecky DR (1985) Heavy metal and sulfur transport during subcritical and supercritical hydrothermal alteration of basalt: Influence of fluid pressure and basalt composition and crystallinity. Geochim Cosmochim Acta 49(12):2545–2560

Smoot NC (1990) Mariana Trough by multi-beam sonar. Geo-Mar Lett 10(3):137–144

Takai K, Horikoshi K (1999) Genetic diversity of archaea in deep-sea hydrothermal vent environments. Genetics 152(4):1285–1297

Tivey MA, Johnson HP (2002) Crustal magnetization reveals subsurface structure of Juan de Fuca Ridge hydrothermal vent fields. Geology 30(11):979–982

Toner BM, Santelli CM, Marcus MA, Wirth R, Chan CS, McCollom T, Bach W, Edwards KJ (2009) Biogenic iron oxyhydroxide formation at mid-ocean ridge hydrothermal vents: Juan de Fuca Ridge. Geochim Cosmochim Acta 73(2):388–403

Tsunogai U, Ishibashi J, Wakita H, Gamo T, Watanabe K, Kajimura T, Kanayama S, Sakai H (1994) Peculiar features of Suiyo Seamount hydrothermal fluids, Izu-Bonin Arc: differences from subaerial volcanism. Earth Planet Sci Lett 126(4):289–301

Tsunogai U, Yoshida N, Ishibashi J, Gamo T (2000) Carbon isotopic distribution of methane in deep-sea hydrothermal plume, Myojin Knoll Caldera, Izu-Bonin arc: implications for microbial methane oxidation in the oceans and applications to heat flux estimation. Geochim Cosmochim Acta 64(14):2439–2452

Tsunogai U, Toki T, Nakayama N, Gamo T, Kato H, Kaneko S (2003) WHATS: a new multi-bottle gas-tight sampler for sea-floor vent fluids (in Japanese with English abstract). Chikyukagaku (Geochem) 37(3):101–109

Urabe T, Maruyama A, Marumo K, Seama N, Ishibashi J (2001) The Archaean park project update. InterRidge News 10(1):23–25

Urabe T, Ishibashi J, Maruyama A, Marumo K, Seama N, Utsumi M (2004) Discovery and drilling of on- and off-axis hydrothermal sites in backarc spreading center of southern Mariana Trough, Western Pacific, paper presented at AGU Fall Meeting. American Geophysical Union V44A-03

Urabe T, Okino S, Sunamura M, Ishibashi J, Takai K, Suzuki K (2009) Trans-crustal advections and in-situ biogeochemical processes of global sub-seafloor aquifer: the sub-seafloor "TAIGA" (in Japanese with English abstract). J Geogr (Chigaku Zasshi) 118 (6):1027–1036

Utsumi M, Tsunogai U, Ishibashi J (2004) Direct measurement of microbial methane oxidation at hydrothermal vent ecosystems, paper presented at AGU 2004 Fall Meeting. American Geophysical Union, V41B-1373, San Francisco

Von Damm KL (1995) Controls on the chemistry and temporal variability of seafloor hydrothermal fluids. In: Humphris SE, Zierenberg RA, Mullineaux LS, Thomson RE (eds) Seafloor hydrothermal systems: physical, chemical, biological, andgeological interactions. American Geophysical Union, Washington DC, pp 222–247

Von Damm KL, Parker CM, Gallant RM, Loveless JP, The AdVenture 9 Science Party (2002) Chemical evolution of hydrothermal fluids from EPR 21° N: 23 years later in a phase separating world. EOS Trans AGU Fall Meet Suppl 83(47) Abstract V61B-1365

Wheat CG, Fryer P, Hulme SM, Becker NC, Curtis A, Moyer C (2003) Hydrothermal venting in the southern most portion of the Mariana backarc spreading centerat 12.57 degrees N, paper presented at AGU Fall Meeting. American Geophysical Union T32A-09020, San Francisco

Yamazaki T, Stern RJ (1997) Topography and magnetic vector anomalies in the Mariana Trough. JAMSTEC J Deep Sea Res 13:31–45

Yamazaki T, Murakami F, Saito E (1993) Mode of seafloor spreading in the northern Mariana Trough. Tectonophysics 221 (2):207–222

Yang K, Scott SD (2006) Magmatic fluids as a source of metals in seafloor hydrothermal systems. In: Back-arc spreading systems: geological, biological, chemical, and physical interactions. AGU, Washington DC, pp 163–184

Yoshikawa S, Okino K, Asada M (2012) Geomorphological variations at hydrothermal sites in the southern Mariana Trough: relationship between hydrothermal activity and topographic characteristics. Mar Geol 303–306:172–182